MATHEMATICAL MODELING AND COMPUTING, Vol. 11, No. 2, pp. 373–384 (2024)

Potential field modeling by combination of near-boundary and contact elements with non-classical finite differences in a heterogeneous medium

Zhuravchak L. M.

Lviv Polytechnic National University,
12 S. Bandera Str., 79013, Lviv, Ukraine

(Received 27 July 2023; Revised 26 March 2024; Accepted 8 April 2024)

In this paper, a generalized scheme for finding solutions of potential theory problems in two-dimensional piecewise-homogeneous media containing local regions with coordinate-dependent physical characteristics has been presented. To describe the additional influence of these local areas, along with the indirect methods of near-boundary and contact elements, a non-classical finite-difference method based on asymmetric finite-difference relations has been used. The software implementation of the developed approach for finding the potential of the direct current electric field in a mountain heterogeneous ridge has been carried out. Approaches to solving elliptic problems that simulate stationary processes in piecewise-homogeneous media with ideal contact conditions at the interfaces and mixed boundary conditions have been considered. They analytically take into account the condition of continuity of the unknown functions (potential, temperature) and are based on the combination of indirect methods of near-boundary and contact elements. Using the software developed, computational experiments have been carried out for the problem of exploration and forecasting of oil and gas deposits in a mountain range by the method of electrical profiling.

Keywords: *indirect near-boundary element method; indirect contact element method; piecewise-homogeneous object; local area of material inhomogeneity; non-classical finite differences; electrical profiling; two-dimensional problem of potential theory.*

2010 MSC: 65N38, 93B18, 80A10 **DOI:** 10.23939/mmc2024.02.373

1. Introduction

When solving potential theory problems, real objects are often modeled with piecewise-homogeneous or heterogeneous media. If the physical characteristics are constant within each zone, it is advisable to use the methods of boundary integral equations [1, 2], in particular, those created on its basis such as boundary [3–8], near-boundary [9], partly-boundary [10] or contact elements [11]. They have a number of indisputable advantages in modeling processes in piecewise-homogeneous media since they allow for the accurate satisfaction of the initial equations of the model, clear description of unrestricted and half-restricted objects, and require only the discretization of boundaries or outer near-boundary zones. They can be considered as variants of the source method and can be attributed to indirect research methods, since the unknown functions entered to solve the problem, are not physical variables.

For media whose physical characteristics depend on an unknown potential, the Kirchhoff transformation is often used [12, 13]. For completely heterogeneous areas in which the physical characteristics of the material continuously depend on the coordinates, researchers use differential methods, in particular, the finite difference method [14–16].

The main difference of the objects considered in this work is that the physical characteristics continuously depend on the coordinates only within some local area of material inhomogeneity (LAMI) of each zone. When constructing a discrete-continuous model of the problem, the advantages of both mentioned approaches have been combined. The differential operator has been split into three operators, the first of which describes a homogeneous environment, the second describes the influence of the media interfaces, the third describes the influence of LAMI. Since the derivatives of the unknown

potential along the coordinates are included in the third operator, they have been approximated by non-classical finite differences at the nodes of the LAMI grid. The indirect method of near-boundary and contact elements and the interpolation of the grid function in the LAMI have been used to construct the integral representation of the solution of Laplace equation. The discrete-continuous model for finding the intensities of unknown sources introduced in near-boundary and contact elements and approximated by constants, and unknown values at grid nodes, is reduced to SLAE, formed as a result of satisfying in the collocational sense of boundary conditions, conditions of ideal contact at the media interfaces and at grid nodes.

The aim of our study is, firstly, to consider stationary processes in objects with inclusions of complex geometric shape that are in ideal contact with the environment and contain LAMI; secondly, to apply the high-precision numerical methods to create a mathematical model; and, thirdly, to estimate the opportunities of the electrical profiling method for exploration and forecasting of conductive objects or oil and gas deposits in mountain ridges.

2. Mathematical model for a piecewise-homogeneous medium with local area of material inhomogeneity of each zone

Let us consider the object, which in the Cartesian coordinate system x_1, x_2 occupies the domain Ω, which contains $M-1$ inclusions Ω_s ($s = 1, \ldots, M-1$, $\Omega \setminus \cup_{s=2}^{M} \Omega_s = \Omega_1$, $\partial\Omega_1 \cap \partial\Omega_s = \partial\Omega_{1s}$, $\partial\Omega_s \cap \partial\Omega = \varnothing$), which are in ideal contact with the medium Ω_1, and local areas of material inhomogeneity $\Omega_{mg} \subset \Omega_m$. Here $\partial\Omega_m$ is a boundary of the domain Ω_m ($m = 1, \ldots, M$).

The conductivity $\lambda(x)$ of such an object, from the point of view of inhomogeneous medium, has been representing:

$$\lambda(x) = \lambda_1 + \sum_{s=2}^{M} (\lambda_s - \lambda_1)\chi_{1s}(x) + \sum_{m=1}^{M} \lambda_{mg}(x)\chi_{mg}, \tag{1}$$

where $\chi_{1s}(x) = 0$ at $x \in \Omega_1$, $\chi_{1s}(x) = 0.5$ for $x \in \partial\Omega_s$, $\chi_{1s}(x) = 1$ for $x \in \Omega_s$; λ_{mg} is a continuous function of Cartesian coordinates x_1, x_2, which approaches zero as $x = (x_1, x_2)$ approaches the boundary $\partial\Omega_{mg}$ of the domain Ω_{mg}, χ_{mg} is a characteristic function of the domain Ω_{mg}.

The unknown functions $u(x)$ have been describing by equations

$$\sum_{i=1}^{2} \frac{\partial}{\partial x_i} \left(\lambda(x) \frac{\partial u(x)}{\partial x_i} \right) = -\psi(x)\chi_1(x), \quad x \in \Omega, \tag{2}$$

boundary conditions of the first and second kinds

$$u(x) = f_{\Gamma}^{(1)}(x), \quad x \in \partial\Omega^{(1)}, \quad -\lambda_1 \frac{\partial u(x)}{\partial \boldsymbol{n}(x)} = f_{\Gamma}^{(2)}(x), \quad x \in \partial\Omega^{(2)}, \tag{3}$$

and conditions of ideal contact at the media interfaces

$$\begin{gathered} u(x)|_{x-0\to\partial\Omega_{1s}} = u(x)|_{x+0\to\partial\Omega_{1s}}, \\ \lambda(x) \left. \frac{\partial u(x)}{\partial \boldsymbol{n}^{1s}(x)} \right|_{x-0\to\partial\Omega_{1s}} = \lambda(x) \left. \frac{\partial u(x)}{\partial \boldsymbol{n}^{1s}(x)} \right|_{x+0\to\partial\Omega_{1s}}, \quad x \in \partial\Omega_{1s}, \quad s = 2, \ldots, M, \end{gathered} \tag{4}$$

where $\boldsymbol{n}(x) = (n_1(x), n_2(x))$, $\boldsymbol{n}^{1s}(x) = (n_1^{1s}(x), \ldots, n_k^{1s}(x))$ are uniquely defined unit normal vectors to $\partial\Omega$ and $\partial\Omega_{1s}$, respectively, when taken $\partial\Omega_{1s}$ as a part of the boundary $\partial\Omega_1$, the records $x - 0 \to \partial\Omega_{1s}$, $x + 0 \to \partial\Omega_{1s}$ indicate that x is directed to $\partial\Omega_1$ from the domains Ω_1, Ω_s, i.e. from left and right; $\partial\Omega^{(1)} \cup \partial\Omega^{(2)} = \partial\Omega$, $\chi_1(x)$ is the characteristic function of the domain Ω_1, that is $\chi_1(x) = 0$ for $x \notin \Omega_1$, $\chi_1(x) = 1$ for $x \in \Omega_1$.

Substituting expression (1) into equation (2) and dividing the latter one by $\lambda(x)$, we obtain the equation for a medium with a conductivity equal to 1 and with sources focused on $\partial\Omega_s$ and in Ω_{mg}, whose intensity is determined by unknown functions $q_j(x) = \partial u(x)/\partial x_j$, $j = 1, 2$:

$$\Delta u(x) = -\sum_{s=2}^{M} D_s \sum_{j=1}^{2} q_j(x) n_j^{1s}(x) \delta\left(x - x|_{\partial\Omega_{1s}}\right) - \sum_{m=1}^{M} \boldsymbol{P}_{mg}(x, u(x)) - \tilde{\psi}(x)\chi_1(x), \quad x \in \Omega, \tag{5}$$

where $D_s = 2\frac{\lambda_1-\lambda_s}{\lambda_1+\lambda_s}$, $\boldsymbol{P}_{mg}(x,u(x)) = \frac{1}{\lambda(x)}\sum_{j=1}^{2}\frac{\partial\lambda_{mg}(x)}{\partial x_j}q_j(x)\chi_{mg}$, $\tilde{\psi}(x) = \frac{\psi(x)}{\lambda(x)}$, Δ is the Laplace operator.

3. Integral representation of the solution

According to the indirect near-boundary element method (INBEM) [9] and indirect contact element methods [11], we introduce "fictitious" sources of unknown intensity $\varphi^{(G)}(x)$, $\varphi_j^{(s)}(x)$, respectively, within the outer, near-boundary to the boundary $\partial\Omega$, zone G and within the interfaces $\partial\Omega_{1s}$, $s = 2,\dots,M$, and describe the unknown function instead of (5) by the equation

$$\Delta u(x) = -\varphi^{(G)}(x)\,\chi_G(x) - \sum_{s=2}^{M} D_s \sum_{j=1}^{2} \varphi_j^{(s)}(x)\, n_j^{1s}(x)\,\chi_{1s}(x) - \sum_{m=1}^{M} \boldsymbol{P}_{mg}(x,u(x)) - \tilde{\psi}(x)\,\chi_1(x), \quad x\in\mathbb{R}^2, \quad (6)$$

where $\chi_G(x)$, $\chi_{1s}(x)$ are the characteristic functions of the domains G and interface $\partial\Omega_{1s}$.

As we can see from (6), such a model automatically ensures the continuity of the potential at an arbitrary point $x\in\partial\Omega_{1s}$ during the transition through the boundary $\partial\Omega_1$, that is, the fulfillment of the first of conditions (4). Thus, we have reduced the problem for solving equation (6) taking into account the boundary conditions (3) and the second one of the contact conditions (4).

Since there is also a well-known fundamental solution (FS) $U(x,\xi)$ for the Laplace operator, we write integral representation of the solution of equation (6) and its coordinate and normal derivatives:

$$\begin{aligned} u(x) &= \boldsymbol{F}^{G\Gamma}(x,U) + \boldsymbol{F}_g(x,U,u) + C + \boldsymbol{F}_\psi(x,U),\\ q_j(x) &= \boldsymbol{F}^{G\Gamma}(x,Q_j) + \boldsymbol{F}_g(x,Q_j,u) + \boldsymbol{F}_\psi(x,Q_j),\\ q(x) &= -\lambda_1\frac{\partial u(x)}{\partial \boldsymbol{n}(x)} = \boldsymbol{F}^{G\Gamma}(x,Q) + \boldsymbol{F}_g(x,Q,u) + \boldsymbol{F}_\psi(x,Q), \end{aligned} \quad (7)$$

where

$$\boldsymbol{F}^{G\Gamma}(x,\Phi) = \int_G \Phi(x,\xi)\varphi^{(G)}(\xi)\,dG(\xi) + \sum_{s=2}^{M} D_s \sum_{j=1}^{2}\int_{\partial\Omega_{1s}} \Phi(x,\xi)\varphi_j^{(s)}(\xi) n_j^{1s}(\xi)\,d\partial\Omega_{1s}(\xi),\ \xi=(\xi_1,\xi_2)\in\mathbb{R}^2,$$

$$\boldsymbol{F}_g(x,\Phi,u) = \sum_{m=1}^{M}\boldsymbol{F}_{mg}(x,\Phi,u), \quad \boldsymbol{F}_{mg}(x,\Phi,u) = \int_{\Omega_{mg}} \boldsymbol{P}_{mg}(\xi,u(\xi))\Phi(x,\xi)\,d\Omega_{mg}(\xi),$$

$$\boldsymbol{F}_\psi(x,\Phi) = \int_{\Omega_1}\Phi(x,\xi)\tilde{\psi}(\xi)\,d\Omega_1(\xi),$$

$Q_j(x,\xi) = \frac{\partial U(x,\xi)}{\partial x_j}$, $Q(x,\xi) = -\lambda_1\sum_{j=1}^{2} Q_j(x,\xi)n_j(x)$, $\Phi\in\{U,Q_j,Q\}$, the constant C appeared as a result of the logarithmic behavior of FS at an infinitely distant point.

Going in (7) x from the middle of the domain Ω to the outer boundary $\partial\Omega$ and to the interfaces $\partial\Omega_{1s}$ to satisfy the boundary conditions (3), we obtain the boundary integral equations (BIE) that connect the unknowns $\varphi^{(G)}(\xi)$, $\varphi_j^{(s)}(x)$ with the given values onto the boundary $u_\Gamma(x)$ and $q_\Gamma(x)$:

$$\begin{aligned} \boldsymbol{F}^{G\Gamma}(x,U) + \boldsymbol{F}_g(x,U,u) + C &= u_\Gamma(x), \quad x\in\partial\Omega^{(1)},\\ \boldsymbol{F}^{G\Gamma}(x,Q) + \boldsymbol{F}_g(x,Q,u) &= q_\Gamma(x), \quad x\in\partial\Omega^{(2)},\\ \boldsymbol{F}^{G\Gamma}(1,1) &= 0. \end{aligned} \quad (8)$$

Note that the last equation reflects the total zero of all sources in Ω.

We supplement them by equations onto $\partial\Omega_{1s}$ and into LAMI:

$$\boldsymbol{F}^{G\Gamma}(x,Q_j) + \boldsymbol{F}_g(x,Q_j,u) - q_j(x) = 0, \quad x\in\partial\Omega_{1s}, \quad (9)$$

$$\boldsymbol{F}^{G\Gamma}(x,U) + \boldsymbol{F}_g(x,U,u) + C - u(x) = 0, \quad x\in\Omega_{mg}. \quad (10)$$

Since it is practically impossible to integrate analytically integrals in system (8)–(10) for the applied problems due to the arbitrary form of domains Ω_m and functions $\varphi^{(G)}(x)$, $\varphi_j^{(s)}(x)$, we can perform

spatial discretization using the following steps. We divide the domains G and $\partial\Omega_{1s}$ into the near-boundary elements of dimension 2 G_v $(v = 1, \dots, V)$ and the contact elements of dimension 1 Γ_l^s $(l = 1, \dots, L_s)$ and approximate unknown functions $\varphi^{(G)}(x)$, $\varphi_j^{(s)}(x)$ into them by quadratic functions $\varphi_v^{(G)}(x)$, $\varphi_{jl}^{(s)}(x)$, which look like [4]:

$$\varphi_v^{(G)}(\xi^{(Gv)}) = \sum_{i=1}^{3} d_v^i f_i(\eta), \quad \varphi_{jl}^{(s)}(\xi^{(sl)}) = \sum_{i=1}^{3} d_{jl}^{si} f_i(\zeta), \tag{11}$$

where $f_1(\eta_i) = 0.5\eta_i(\eta_i - 1)$, $f_2(\eta_i) = 1 - \eta_i^2$, $f_3(\eta_i) = 0.5\eta_i(\eta_i + 1)$.

It is clear that $\cup_{v=1}^{V} G_v = G$, $\cup_{l=1}^{L_s} \Gamma_l^s = \partial\Omega_{1s}$, the intensity of the unknown source into the thickness and height of the near-boundary element does not change, the same is into the thickness of the contact element. We used Lagrangian elements because the extra internal nodes significantly improve the results.

After spatial discretization, taking into account (11), instead of (7) we have:

$$\begin{aligned}
u(x) &= \sum_{v=1}^{V}\sum_{i=1}^{3} A_v^{Gi}(x,U)d_v^i + \sum_{s=2}^{M} D_s \sum_{l=1}^{L_s}\sum_{i=1}^{3} A_l^{si}(x,U)\sum_{b=1}^{2} d_{bl}^{si} n_{bl}^{1si} + \boldsymbol{F}_g(x,U,u) + C + \boldsymbol{F}_\psi(x,U),\\
q_j(x) &= \sum_{v=1}^{V}\sum_{i=1}^{3} A_v^{Gi}(x,Q_j)d_v^i + \sum_{s=2}^{M} D_s \sum_{l=1}^{L_s}\sum_{i=1}^{3} A_l^{si}(x,Q_j)\sum_{b=1}^{2} d_{bl}^{si} n_{bl}^{1si} + \boldsymbol{F}_g(x,Q_j,u) + \boldsymbol{F}_\psi(x,Q_j),\\
q(x) &= \sum_{v=1}^{V}\sum_{i=1}^{3} A_v^{Gi}(x,Q)d_v^i + \sum_{s=2}^{M} D_s \sum_{l=1}^{L_s}\sum_{i=1}^{3} A_l^{si}(x,Q)\sum_{b=1}^{k} d_{bl}^{si} n_{bl}^{1si} + \boldsymbol{F}_g(x,Q,u) + \boldsymbol{F}_\psi(x,Q),
\end{aligned} \tag{12}$$

where

$$A_v^{Gi}(x,\Phi) = \int_{-1}^{+1}\int_{-1}^{+1} \Phi\big(x,\xi^{(Gv)}\big)\,\big|J_2\big(\xi^{(Gv)},\eta\big)\big|\,f_i(\eta)\,d\eta_1\,d\eta_2,$$

$$A_l^{si}(x,\Phi) = D_s\int_{-1}^{+1} \Phi\big(x,\xi^{(sl)}\big)\,\big|J_1\big(\xi^{(sl)},\zeta\big)\big|\,f_i(\zeta)\,d\zeta,$$

$J_2(\xi,\eta)$ and $J_1(\xi,\zeta)$ are Jacobians of transition from variables ξ to η and from ξ to ζ, respectively; n_{jl}^{1si} is the value of the normal in i-th node of l-th contact element, which belongs to $\partial\Omega_{1s}$. Note that the integrals $A_v^{Gi}(x,U)$, $A_v^{Gi}(x,Q_j)$, $A_v^{Gi}(x,Q)$, $A_l^{si}(x,U)$ for $\xi = x$ contain a singular feature, and the integrals $A_l^{si}(x,Q_j)$, $A_l^{si}(x,Q)$ are calculated in the Cauchy sense.

4. Approximation of derivatives of the unknown potential into LAMI

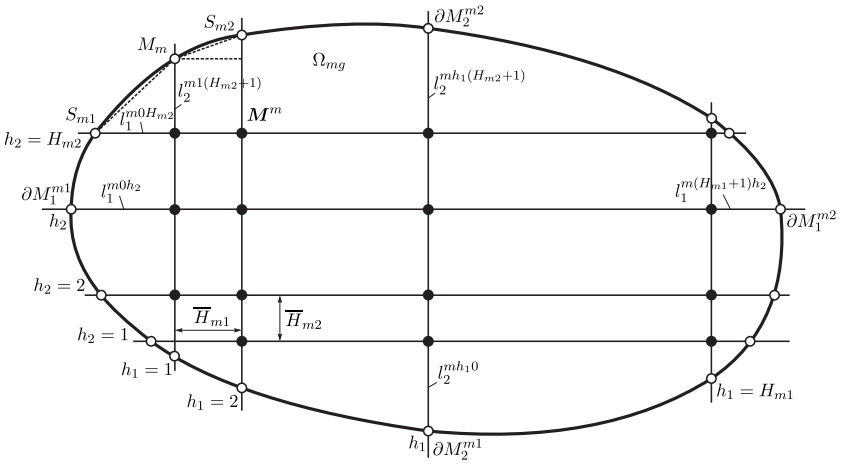

Fig. 1. The grid into LAMI.

Since the operator $\boldsymbol{F}_{mg}(x,\Phi,u)$ includes unknown first derivatives of the coordinates of the potential, in the regions Ω_{mg} we use classical and non-classical finite differences and interpolation of unknown functions.

In each region Ω_{mg} we will draw lines $L_{h_2}^{m2}$, $L_{h_1}^{m1}$ $(h_i = 1, \dots, H_{mi}, i = 1, 2, H_{mi}$ are odd numbers), parallel to the axes x_1, x_2, with steps $\bar{H}_{m2}$, $\bar{H}_{m1}$, that will cover it with an uneven grid (Figure 1).

Grid nodes are defined by pairs of numbers $(h_1,\ h_2)$, in particular, for internal $\boldsymbol{M}^m = \{L^{mh_1h_2}\colon h_i = 1, \dots, H_{mi}\}$ and for

boundary ($L^{mh_1h_2} \in \partial \boldsymbol{M}^m = \cup_{i=1}^{2} \cup_{t=1}^{2} \partial M_i^{mt}$) one of these numbers is equal to 0 or $H_{mi}+1$, and the other two ones change from 1 to H_{mi}:

$$\partial M_1^{m1} = \left\{L^{m0h_2}\right\}, \quad \partial M_1^{m2} = \left\{L^{m(H_{m1}+1)h_2}\right\}, \quad h_2 = 1, \ldots, H_{m2},$$
$$\partial M_2^{m1} = \left\{L^{mh_10}\right\}, \quad \partial M_2^{m2} = \left\{L^{mh_1(H_{m2}+1)}\right\}, \quad h_1 = 1, \ldots, H_{m1}.$$

To write the grid function of the operator $\boldsymbol{P}_{mg}(\xi, u(\xi, \xi_4))$, we approximate $\partial u(\xi)/\partial x_i$ by $u^{mh_1h_2} = u(\xi^{L_m})$ ($\xi^{L_m} = \xi^{mh_1h_2} = (\xi_1^{mh_1h_2}, \xi_2^{mh_1h_2})$ are the coordinates of grid nodes), applying non-classical and classical finite differences. Therefore, $u^{mh_1h_2}$ corresponds to the value of the desired function at the point $L^{mh_1h_2}$.

To find the values of the derivatives in the internal nodes, we use the central differences:

$$\frac{\partial u(\xi^{mh_1h_2})}{\partial x_1} = \frac{u^{m(h_1+1)h_2} - u^{m(h_1-1)h_2}}{2\bar{H}_{m1}}, \quad h_1 = 2, \ldots, H_{m1}-1,$$
$$\frac{\partial u(\xi^{mh_1h_2})}{\partial x_2} = \frac{u^{mh_1(h_2+1)} - u^{mh_1(h_2-1)}}{2\bar{H}_{m2}}, \quad h_2 = 2, \ldots, H_{m2}-1,$$
$$\frac{\partial u(\xi^{m1h_2})}{\partial x_1} = \frac{1}{2}\left(\frac{u^{m1h_2} - u^{m0h_2}}{l_1^{m0h_2}} + \frac{u^{m2h_2} - u^{m1h_2}}{\bar{H}_{m1}}\right),$$
$$\frac{\partial u(\xi^{mH_1h_2})}{\partial x_1} = \frac{1}{2}\left(\frac{u^{m(H_{m1}+1)h_2} - u^{mH_{m1}h_2}}{l_1^{m(H_{m1}+1)h_2}} + \frac{u^{m(H_{m1}+1)h_2} - u^{mH_{m1}h_2}}{\bar{H}_{m1}}\right),$$
$$\frac{\partial u(\xi^{mh_11})}{\partial x_2} = \frac{1}{2}\left(\frac{u^{mh_11} - u^{mh_10}}{l_2^{mh_10}} + \frac{u^{mh_12} - u^{mh_11}}{\bar{H}_{m2}}\right),$$
$$\frac{\partial u(\xi^{mh_1H_{m2}})}{\partial x_2} = \frac{1}{2}\left(\frac{u^{mh_1(H_{m2}+1)} - u^{mh_1H_{m2}}}{l_2^{mh_1(H_{m2}+1)}} + \frac{u^{mh_1(H_{m2}+1)} - u^{mh_1H_{m2}}}{\bar{H}_{m2}}\right),$$

where $l_1^{m0h_2} = x_1^{m1h_2} - x_1^{m0h_2}$, $l_1^{m(H_{m1}+1)h_2} = x_1^{m(H_{m1}+1)h_2} - x_1^{mH_{m1}h_2}$, $l_2^{mh_10} = x_2^{mh_11} - x_2^{mh_10}$, $l_2^{mh_1(H_{m2}+1)} = x_2^{mh_1(H_{m2}+1)} - x_2^{mh_1H_{m2}}$.

For boundary nodes belonging to ∂M_i^{mt}, the value of the i-th derivative is determined by right or left differences, respectively:

$$\frac{\partial u(\xi^{m0h_2})}{\partial x_1} = \frac{u^{m1h_2} - u^{m0h_2}}{l_1^{m0h_2}}, \quad \frac{\partial u(\xi^{m(H_{m1}+1)h_2})}{\partial x_1} = \frac{u^{m(H_{m1}+1)h_2} - u^{mH_{m1}h_2}}{l_1^{m(H_{m1}+1)h_2}},$$
$$\frac{\partial u(\xi^{mh_10})}{\partial x_2} = \frac{u^{mh_11} - u^{mh_10}}{l_2^{mh_10}}, \quad \frac{\partial u(\xi^{mh_1(H_{m2}+1)})}{\partial x_2} = \frac{u^{mh_1(H_{m2}+1)} - u^{mh_1H_{m2}}}{l_2^{mh_1(H_{m2}+1)}}.$$

The value of the j-th derivative ($j \neq i$) is expressed in terms of the value at this node and at the two boundary nodes S_{m2}, S_{m1} closest to it in the positive and negative directions of the axis Ox_j:

$$\frac{\partial u(\xi^{mh_1h_2})}{\partial x_j} = \frac{1}{2}\left(\left(u^{mS_{m2}} - u^{mh_1h_2}\right)H_{jS_{m2}}^{mih_1h_2} + \left(u^{mh_1h_2} - u^{mS_{m1}}\right)H_{jS_{m1}}^{mih_1h_2}\right), \ \xi^{mh_1h_2} \in \partial M_i^{m1} \cup \partial M_i^{m2},$$

where

$$H_{jS_{mk}}^{mih_1h_2} = H_{ih_1h_2}^{mjS_{mk}} = H_j^{mih_1h_2} = \frac{\bar{H}_{mj}}{\bar{H}_{mj}^2 + (\xi_i^{mS_{mk}} - \xi_i^{mh_1h_2})^2} \quad \text{for} \quad S_{mk} \in \partial M_i^{mt}, \quad k = 1, 2,$$

$$S_{m2} = \left\{ \begin{array}{c} 0 \\ H_{m1}+1 \end{array} \right\}(h_2+1), \quad S_{m1} = \left\{ \begin{array}{c} 0 \\ H_{m1}+1 \end{array} \right\}(h_2-1) \quad \text{for} \quad i = 1, \ j = 2, \quad t = \left\{ \begin{array}{c} 1 \\ 2 \end{array} \right.,$$

$$S_{m2} = (h_1+1)\left\{ \begin{array}{c} 0 \\ H_{m2}+1 \end{array} \right\}, \quad S_{m1} = (h_1-1)\left\{ \begin{array}{c} 0 \\ H_{m2}+1 \end{array} \right\} \quad \text{for} \quad i = 2, \ j = 1, \quad t = \left\{ \begin{array}{c} 1 \\ 2 \end{array} \right.,$$

$$H_{jS_{mk}}^{mih_1h_2} = \frac{|\xi_j^{mh_1h_2} - \xi_j^{mS_{mk}}|}{(\xi_j^{mh_1h_2} - \xi_j^{mS_{mk}})^2 + (\xi_i^{mh_1h_2} - \xi_i^{mS_{mk}})^2} \quad \text{for} \quad S_{mk} \in \partial M_j^{mz},$$

$$S_{m2}=H_{m1}\left\{\begin{array}{c}0\\ H_{m2}+1\end{array}\right\},\quad S_{m1}=1\left\{\begin{array}{c}0\\ H_{m2}+1\end{array}\right\}\quad \text{for}\quad i=1,\ j=2,\quad z=\left\{\begin{array}{c}1\\ 2\end{array}\right.,$$

$$S_{m2}=\left\{\begin{array}{c}0\\ H_{m1}+1\end{array}\right\}H_{m2},\quad S_{m1}=\left\{\begin{array}{c}0\\ H_{m1}+1\end{array}\right\}1\quad \text{for}\quad i=2,\ j=1,\quad z=\left\{\begin{array}{c}1\\ 2\end{array}\right..$$

Using classical and non-classical finite differences in the operator $\boldsymbol{P}_{mg}(\xi,u^{(m)}(\xi))$, we obtain the grid function

$$\psi_g^{(m)}(\xi^{mM})=\frac{1}{2}\sum_{h_1h_2\in M^m\cup\partial M^m}\gamma^{mh_1h_2}u^{mh_1h_2},\tag{13}$$

where $\gamma^{mh_1h_2}=\gamma_1^{h_1h_2}(\Lambda_1^{mh_1h_2})+\gamma_2^{h_1h_2}(\Lambda_2^{mh_1h_2})$, $\xi^{mM}\in M^m\cup\partial M^m$, $\Lambda_i^{mh_1h_2}=\frac{1}{\lambda^{(m)}(\xi^{mh_1h_2})}\frac{\partial\lambda_{mg}(\xi^{mh_1h_2})}{\partial x_i}$.

For the points of the sets ∂M_2^{m1} ($h_2=0$, $i=2$), ∂M_2^{m2} ($h_2=H_{m2}+1$, $i=2$) the functions $\gamma_1^{mh_1h_2}(\Lambda^m)$ have the form

$$\left\{\begin{array}{c}-H_1^{m21h_2}\big(\Lambda^{m1h_2}+\Lambda^{m2h_2}\big)+H_{10(h_2\pm1)}^{m21h_2}\Lambda^{m1h_2},\quad h_1=1,\\ H_1^{m2(h_1-1)h_2}\big(\Lambda^{m(h_1-1)h_2}+\Lambda^{mh_1h_2}\big)-H_1^{m2h_1h_2}\big(\Lambda^{m(h_1+1)h_2}+\Lambda^{mh_1h_2}\big),\quad h_1=2,\dots,H_{m1}-1,\\ H_1^{m2(H_1-1)h_2}\big(\Lambda^{mH_1h_2}+\Lambda^{m(H_1-1)h_2}\big)-\Lambda^{mH_1h_2},\quad h_1=H_{m1},\\ \big(H_{10(h_2\pm1)}^{m21h_2}-H_{12(h_2\pm1)}^{m21h_2}\big)\Lambda^{m1h_2},\quad H_{m1}=1,\end{array}\right.$$

and the functions $\gamma_2^{mh_1h_2}(\Lambda^m)$ for nodes of ∂M_1^{m1} ($h_1=0$, $i=1$), ∂M_1^{m2} ($h_1=H_{m1}+1$, $i=1$) are as follows:

$$\left\{\begin{array}{c}-H_2^{m1h_11}\big(\Lambda^{mh_11}+\Lambda^{mh_12}\big)+H_{2(h_1\pm1)0}^{m1h_11}\Lambda^{mh_11},\quad h_2=1,\\ H_2^{m1h_1(h_2-1)}\big(\Lambda^{mh_1h_2}+\Lambda^{mh_1(h_2-1)}\big)-H_2^{m1h_1h_2}\big(\Lambda^{mh_1h_2}+\Lambda^{mh_1(h_2+1)}\big),\quad h_2=2,\dots,H_{m2}-1,\\ H_2^{m1h_1(H_2-1)}\big(\Lambda^{mh_1H_2}+\Lambda^{mh_1(H_2-1)}\big)-H_{2(h_1\pm1)(H_2+1)}^{m1h_1H_2}\Lambda^{mh_1H_2},\quad h_2=H_{m2},\\ \big(H_{2(h_1\pm1)0}^{m1h_11}-H_{2(h_1\pm1)2}^{m1h_11}\big)\Lambda^{mh_11},\quad H_{m2}=1,\end{array}\right.$$

here the sign "+" in the expressions $h_i\pm1$ is chosen for the points of the sets ∂M_i^{m1} and the sign "−" — for the points of the sets ∂M_i^{m2}.

For the points of the sets ∂M_i^{m1}, ∂M_i^{m2}, we obtain the functions $\gamma_i^{mh_1h_2}(\Lambda)$ in the form:

$$\gamma_1^{m0h_2}(\Lambda)=-\frac{2\Lambda^{0h_2}+\Lambda^{1h_2}}{l_1^{m0h_2}}-\delta_{1h_2}H_{101}^{210}\Lambda^{10}-\delta_{H_2h_2}H_{10H_2}^{21(H_2+1)}\Lambda^{1(H_2+1)},\quad L_m\in\partial M_1^{m1},$$

$$\gamma_1^{m(H_1+1)h_2}(\Lambda^m)=\frac{2\Lambda^{m(H_1+1)h_2}+\Lambda^{mH_1h_2}}{l_1^{m(H_1+1)h_2}}+\delta_{1h_2}H_{1(H_1+1)1}^{m2H_10}\Lambda^{mH_10}+\delta_{H_2h_2}H_{1(H_1+1)H_2}^{m2H_1(H_2+1)}\Lambda^{mH_1(H_2+1)},\quad L_m\in\partial M_1^{m2},$$

$$\gamma_2^{mh_10}(\Lambda^m)=-\frac{2\Lambda^{mh_10}+\Lambda^{mh_11}}{l_2^{mh_10}}-\delta_{1h_1}H_{210}^{m101}\Lambda^{m01}-\delta_{H_1h_1}H_{2H_10}^{m1(H_1+1)1}\Lambda^{m(H_1+1)1},\quad L_m\in\partial M_2^{m1},$$

$$\gamma_2^{mh_1(H_2+1)}(\Lambda^m)=\frac{2\Lambda^{mh_1(H_2+1)}+\Lambda^{mh_1H_2}}{l_2^{mh_1(H_2+1)}}+\delta_{1h_1}H_{210}^{m10H_2}\Lambda^{m0H_2}+\delta_{H_1h_1}H_{2H_1(H_2+1)}^{m1(H_1+1)H_2}\Lambda^{m(H_1+1)H_2},\quad L_m\in\partial M_2^{m2}.$$

For the central points ($L_m\in M^m$) the functions have the form:

$$\gamma_1^{h_1h_2}(\Lambda)=\left\{\begin{array}{l}-\dfrac{\Lambda^{1h_2}+\Lambda^{2h_2}}{\bar H_{m1}}+\dfrac{2\Lambda^{0h_2}+\Lambda^{1h_2}}{l_1^{m0h_2}},\quad h_1=1,\\ \dfrac{\Lambda^{(h_1-1)h_2}-\Lambda^{(h_1+1)h_2}}{\bar H_{m1}},\quad h_1=2,\dots,H_{m1}-1,\\ \dfrac{\Lambda^{H_1h_2}+\Lambda^{(H_{m1}-1)h_2}}{\bar H_{m1}}-\dfrac{2\Lambda^{(H_{m1}+1)h_2}+\Lambda^{H_{m1}h_2}}{l_1^{m(H_{m1}+1)h_2}},\quad h_1=H_{m1},\\ \dfrac{2\Lambda^{0h_2}+\Lambda^{1h_2}}{l_1^{m0h_2}}-\dfrac{2\Lambda^{2h_2}+\Lambda^{1h_2}}{l_1^{m2h_2}},\quad H_{m1}=1,\end{array}\right.$$

$$\gamma_2^{h_1h_2}(\Lambda)=\begin{cases}-\dfrac{\Lambda^{h_11}+\Lambda^{h_12}}{\bar H_{m2}}+\dfrac{2\Lambda^{h_10}+\Lambda^{h_11}}{l_2^{mh_10}}, & h_2=1,\\ \dfrac{\Lambda^{h_1(h_2-1)}-\Lambda^{h_1(h_2+1)}}{\bar H_{m2}}, & h_2=2,\dots,H_{m2}-1,\\ \dfrac{\Lambda^{h_1H_2}+\Lambda^{h_1(H_{m2}-1)}}{\bar H_{m2}}-\dfrac{2\Lambda^{h_1(H_{m2}+1)}+\Lambda^{h_1H_{m2}}}{l_2^{mh_1(H_{m2}+1)}}, & h_2=H_{m2},\\ \dfrac{2\Lambda^{h_10}+\Lambda^{h_11}}{l_2^{mh_10}}-\dfrac{2\Lambda^{h_12}+\Lambda^{h_11}}{l_2^{mh_12}}, & H_{m2}=1.\end{cases}$$

5. The SLAE construction for finding unknown values entered in near-boundary elements, contact elements and in grid nodes

To interpolate the operator $F_{mg}(x,\Phi,u)$ according to its grid function (13) by quadratic Lagrangian quadrilateral elements with 9 nodes, we introduce on $\partial\Omega_{mg}$ four additional points $(0,0)$, $(H_{m1}+1,0)$, $(H_{m1}+1,H_{m2}+1)$, $(0,H_{m2}+1)$ respectively between the boundary nodes of the grid with numbers $(0,1)$ and $(1,0)$, $(H_{m1},0)$ and $(H_{m1}+1,1)$, $(H_{m1},H_{m2}+1)$ and $(H_{m1}+1,H_{m2})$, $(0,H_{m2})$ and $(1,H_{m2}+1)$. This will allow us to distinguish in the region $\Omega_{mg}\cup\partial\Omega_{mg}$ curvilinear subregions $\Omega_{mg}^{l_1l_2}$ such that $\Omega_{mg}\cup\partial\Omega_{mg}=\cup_{l_2}^{L_{m2}}\cup_{l_1}^{L_{m1}}\Omega_{mg}^{l_1l_2}$. Here $l_i=[h_i/2]+1$ for $h_i=0,1,(2),H_{mi}$, $l_i=h_i/2$ for $h_i=2,(2),H_{mi}+1$, $L_i=[H_{mi}/2]+1$, $i=1,2$. The record $h_i=a,(2),b$ means that h_i changes from a to b with a step of 2, $[a]$ is integer part of a.

Next, we will use 3×3 nodes of the extended grid to describe the geometry of the subdomain $\Omega_{mg}^{l_1l_2}$ and for interpolation in it, and we will move from the global coordinate system to the local coordinate system η_1,η_2 within $\Omega_{mg}^{l_1l_2}$. Then instead $\boldsymbol{F}_{mg}(x,\Phi,u)$ we get

$$\boldsymbol{I}_g^{(m)}(x,\Phi,u^{m\boldsymbol{M}})=\frac{1}{2}\sum_{h_1=0}^{H_{m1}+1}\sum_{h_2=0}^{H_{m2}+1}\beta^{mh_1h_2}(x,\Phi)\gamma^{mh_1h_2}u^{mh_1h_2},$$

where the appearance of the function $\beta^{mh_1h_2}(\Phi)$ depends on the location of the node h_1h_2.

In boundary nodes with one odd index and additional ones, as well as internal nodes with two odd indices, the function has one term: $\beta^{mh_1h_2}(x,\Phi)=\alpha_{b_1b_2}^{ml_1l_2}(x,\Phi)$, $b_i=2$ for $h_i=1,(2),H_{mi}$, $b_i=1$ for $h_i=0$, $M\in\partial M_i^1$, $b_i=3$ for $h_i=H_{mi}+1$, $M\in\partial M_i^2$.

For boundary and internal nodes with one even index the function has two terms: $\beta^{mh_1h_2}(x,\Phi)=\alpha_{3b_2}^{m(h_1/2)l_2}(x,\Phi)+\alpha_{1b_2}^{m((h_1+1)/2)l_2}(x,\Phi)$, h_2 is odd number, 0 or $H_{m2}+1$, $\beta^{mh_1h_2}(x,\Phi)=\alpha_{b_13}^{ml_1(h_2/2)}(x,\Phi)+\alpha_{b_11}^{ml_1((h_2+1)/2)}(x,\Phi)$, h_1 is odd number, 0 or $H_{m1}+1$.

For internal nodes with two even indices the function has four terms:

$$\beta^{mh_1h_2}(x,\Phi)=\alpha_{33}^{m(h_1/2)(h_2/2)}(x,\Phi)+\alpha_{13}^{m((h_1+1)/2)(h_2/2)}(x,\Phi)+\alpha_{31}^{m(h_1/2)((h_2+1)/2)}(x,\Phi)+\alpha_{11}^{m((h_1+1)/2)((h_2+1)/2)}(x,\Phi).$$

Here $\alpha_{b_1b_2}^{ml_1l_2}(x,\Phi)=\Phi(x,\xi^{ml_1l_2}(\eta_1,\eta_2))\,\phi_{b_1b_2}(\eta_1,\eta_2)\,|J_2(\xi^{ml_1l_2},\eta)|$, $-1\leqslant\eta_i\leqslant1$, $\phi_{b_1b_2}(\eta_1,\eta_2)=f_{b_1}(\eta_1)f_{b_2}(\eta_2)$, $b_i=1,2,3$, $i=1,2$.

We construct a system of linear algebraic equations (SLAE) to determine the nodal values using the weighted residuals method for boundary conditions and for conditions at the interface. We satisfy the BIE (8) at the collocation points belonging to the boundary elements and add the conditions of coincidence of the unknown constants d_{jl}^{si} with $q_j(x^t)$, calculated by the second of formulas (12), at the nodes of the contact elements. We also use the collocation method to satisfy the coincidence conditions u^{mt} $(t=(t_1,t_2))$ with $u(x^{mt})$ at the nodes of the extended grid. The collocation points were chosen as the beginning, the center of mass, and the end of the boundary or contact element.

After finding the unknown constants d_v^i, d_{bl}^{si}, u^{mt} from the SLAE, we determine the potential $u(x)$ and the flow $q(x)$ by formulas (12) at the points of observation inside the object, at the interfaces and at the outer boundary.

6. Finding the potential of the DC electric field in a mountain ridge with LAMI

Suppose that $\Omega \subset \Omega^M$, where the domain Ω^M is an unbounded right angle, which we describe with two rays $P_1 = \{(x_1, x_2)\colon 0 \leqslant x_1 < \infty, x_2 = 0\}$ and $P_2 = \{(x_1, x_2)\colon -\infty < x_2 < 0, x_1 = 0\}$ (Figure 2). We denote the parts of the boundary $\partial\Omega$ coinciding with P_1, P_2, respectively, N_1, N_2. We describe the part of the boundary $N_3 = \partial\Omega\backslash(\cup_{i=1}^2 N_i)$ by the known curve $x_2 = f(x_1)$. The boundary conditions were set as follows:

$$-\sigma_1 \frac{\partial u(x)}{\partial \boldsymbol{n}(x)} = q^{(i)}(x), \quad x \in N_i, \quad i = 1,2,3, \quad u^{(1)}(x) = 0, \quad x \in N_4, \tag{14}$$

moreover, $\sum_{i=1}^3 \int_{N_i} q^{(i)}(x)\, dN_i(x) = 0$. Note that the choice of sources on the rays P_1, P_2 in the form $\tilde{\psi}(x) = \frac{2}{\sigma_1}(q^{(1)}(x) + q^{(2)}(x))$ ensures that conditions (14) are satisfied on N_1, N_2.

According to INBEM, we consider the domain $B \supset \Omega$, $B \subset \mathbb{R}^2$, $\partial\Omega \cap \partial B = \cup_{i=1}^2 N_i$. Assume that the distance between the curves ∂B and N_3 is sufficient to accommodate the near-boundary elements. We define the potential and its coordinates and normal derivatives by formulas similar to (12) without addition with unknown C, taking into account a special fundamental solution U_z for a right angle instead of FS for a plane and such an expression for

$$\boldsymbol{F}_\psi(x,\Phi) = \frac{2}{\sigma_1}\sum_{i=1}^{2}\int_{N_i} q^{(i)}(x)\,\Phi(x,\xi)\,dN_i(\xi), \quad \Phi_z(x,\xi) = \sum_{i=1}^{2}\Big(\Phi(x,\xi^{(i)}) + \Phi(x,\xi'^{(i)})\Big),$$
$$\xi^{(1)} = (\xi_1,\xi_2), \quad \xi'^{(1)} = (\xi_1,-\xi_2), \quad \xi^{(2)} = (-\xi_1,\xi_2), \quad \xi'^{(2)} = (-\xi_1,-\xi_2).$$

The peculiarity of the proposed approach is that we satisfy boundary conditions (14) only on N_3, N_4 and on N_1, N_2 they are fulfilled automatically.

The functions in boundary conditions (14) were as follows:

$$q^{(1)}(x) = 0.5\big(\delta(x_1 - 16) - \delta(x_1 - 20)\big), \quad q^{(2)}(x) = 0, \quad q^{(3)}(x) = 0,$$
$$N_3 = \big\{(x_1,x_2)\colon 0 < x_1 < 2.5, x_2 = f(x_1)\big\}, \quad N_4 = \big\{(x_1,x_2)\colon 2.5 \leqslant x_1 < 3, x_2 = f(x_1)\big\},$$

$f(x_1) = 2x_1^2/3 - 11x_1/3 + 5$ for $0 < x_1 < 3$.

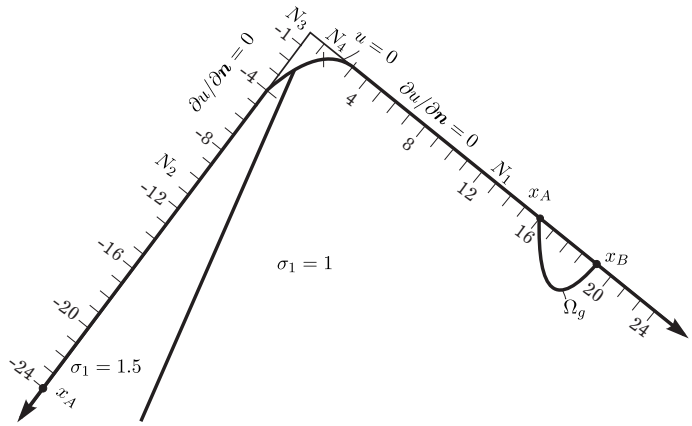

Fig. 2. The model of a mountain ridge with LAMI.

Electrical conductivities were specified by formulas

$$\sigma^{(1)}(\xi) = \sigma_1 + \sigma_g(\xi)\chi_g,\ \sigma_1 = 1,$$
$$\sigma^{(2)}(\xi) = \sigma_2 = 1.5,$$

in which $\sigma_g(\xi)$ was a function of two parameters

$$\sigma_g(\xi_1,\xi_2) = \big(1-\xi_1^2\big)\big(1-\xi_2^2\big)k_\sigma.$$

At the same time, the relationship between the coordinates ξ_1, ξ_2 and η_1, η_2 was written by the formula

$$\xi_i^{l_1 l_2}(\eta_1,\eta_2) = \sum_{b_1=1}^{3}\sum_{b_2=1}^{3}\phi_{b_1 b_2}(\eta_1,\eta_2)\,\xi_i^{b_1 b_2},$$

where $\xi_1^{11} = 17.2$, $\xi_1^{21} = \xi_1^{22} = \xi_1^{32} = 18$, $\xi_1^{31} = 19.35$, $\xi_1^{12} = 16.75$, $\xi_1^{13} = 16.65$, $\xi_1^{23} = 19.25$, $\xi_1^{33} = 18.8$, $\xi_2^{11} = -\xi_2^{33} = -0.8$, $\xi_2^{21} = -\xi_2^{32} = -1.25$, $\xi_2^{31} = -\xi_2^{13} = -1.35$, $\xi_2^{12} = \xi_2^{22} = \xi_2^{23} = 0$, here the index $m = 1$ is omitted.

The potential and its derivative along the normal were determined by formulas similar to (12), taking into account the Green's function U_z for a right angle instead of the FS:

$$u(x) = \sum_{v=1}^{V}\sum_{i=1}^{3} A_v^{Gi}(x,U_z)d_v^i + \sum_{s=2}^{M} D_s \sum_{l=1}^{L_s}\sum_{i=1}^{3} A_l^{si}(x,U_z)\sum_{b=1}^{2} d_{bl}^{si} n_{bl}^{1si}$$
$$+ \frac{1}{2}\sum_{h_1=0}^{H_1+1}\sum_{h_2=0}^{H_2+1}\beta^h(x,U_z)\gamma^h u^h + \boldsymbol{I}_2(x,U_z),$$

$$q_j(x) = \sum_{v=1}^{V}\sum_{i=1}^{3} A_v^{Gi}(x, Q_{zj}) d_v^i + \sum_{s=2}^{M} D_s \sum_{l=1}^{L_s}\sum_{i=1}^{3} A_l^{si}(x, Q_{zj}) \sum_{b=1}^{2} d_{bl}^{si} n_{bl}^{1si} + \frac{1}{2}\sum_{h_1=0}^{H_1+1}\sum_{h_2=0}^{H_2+1} \beta^h(x, Q_{zj})\gamma^h u^h + \boldsymbol{I}_2(x, Q_{zj}),$$

$$q(x) = \sum_{v=1}^{V}\sum_{i=1}^{3} A_v^{Gi}(x, Q) d_v^i + \sum_{s=2}^{M} D_s \sum_{l=1}^{L_s}\sum_{i=1}^{3} A_l^{si}(x, Q) \sum_{b=1}^{k} d_{bl}^{si} n_{bl}^{1si} + \frac{1}{2}\sum_{h_1=0}^{H_1+1}\sum_{h_2=0}^{H_2+1} \beta^h(x, U_z)\gamma^h u^h + \boldsymbol{I}_2(x, U_z),$$

where

$$\boldsymbol{I}_2(x, \Phi) = \frac{2}{\sigma_1}\sum_{i=1}^{2}\int_{N_i} q^{(i)}(\xi)\,\Phi(x, \xi)\,dN_i(\xi).$$

The required accuracy was achieved for 21 grid nodes, i.e. for $H_1 = H_2 = 3$. The accuracy of the numerical integration on the near-boundary elements and on the discretization elements of the domains Ω_{gl} was controlled as follows: the value of the integral on the element was compared with the sum of the values of the integrals on its four components.

Since one of the main types of field observations for direct current methods is electrical profiling by the method of removing median gradients, we will calculate the apparent resistivity ρ_1 of the medium (the value reversed to its conductivity σ_1) by the formula: $\rho_a = k_u|u(x_N) - u(x_M)|$, where k_u is the normal gradient setting factor: $k_u = \pi\left(\ln\frac{R_{AM}R_{BN}}{R_{AN}R_{BM}}\right)^{-1}$ for a half space, $k_u = 1/U_z(x_M, x_A) - 1/U_z(x_M, x_B) + 1/U_z(x_N, x_B) - 1/U_z(x_N, x_A)$ for a right angle, M and N are moving observation points on $\partial\Omega$, between which the potential difference was determined, A and B are the points at which fixed real power sources with intensity $\delta(x - x_A)$ and $(-1)\delta(x - x_B)$ were placed.

In the Table 1 we compared the apparent resistivity, calculated using contact elements and analytically, for a conventional gradient installation over a vertical contact of two media in a half space for $\rho_0 = 4$, $\rho_1 = 1$, $x_A = (-5; 0)$, $x_B = (5; 0)$.

Table 1.

x_1	Analytical solution	Contact elements	x_1	Analytical solution	Contact elements	x_1	Analytical solution	Contact elements
−4.00	3.999	3.999	−1.25	4.000	3.991	1.50	0.999	1.009
−3.75	4.000	3.993	−1.00	4.000	3.991	1.75	1.001	1.009
−3.50	4.005	3.989	−0.75	4.001	3.990	2.00	1.001	1.009
−3.25	4.005	3.996	−0.50	4.001	3.992	2.25	1.000	1.009
−3.00	3.994	3.994	−0.25	4.000	3.930	2.50	1.000	1.008
−2.75	3.997	3.997	0.00	2.500	2.499	2.75	1.000	1.007
−2.50	4.007	3.995	0.25	1.000	1.070	3.00	1.000	1.006
−2.25	4.000	3.988	0.50	1.000	1.010	3.25	0.999	1.006
−2.00	3.996	3.991	0.75	1.000	1.010	3.50	1.000	1.005
−1.75	4.002	3.993	1.00	1.000	1.009	3.75	1.000	1.004
−1.50	4.000	3.990	1.25	0.999	1.009	4.00	1.000	1.003

Numerical results showed (Figure 3) that with a given location of inhomogeneity, source and drain at the boundary $\partial\Omega^M$, in Ω_g and in the area adjacent to it, there is concentration of equipotential lines when electrical conductivity increases in Ω_g.

We have the opposite effect with low-impedance LAMI, in this case equipotential lines are located less often. The effect of torsion of the specified lines is also observed, the direction of which depends on the sign of the value k_σ, but it is visually manifested somewhat worse than thickening or rarefaction.

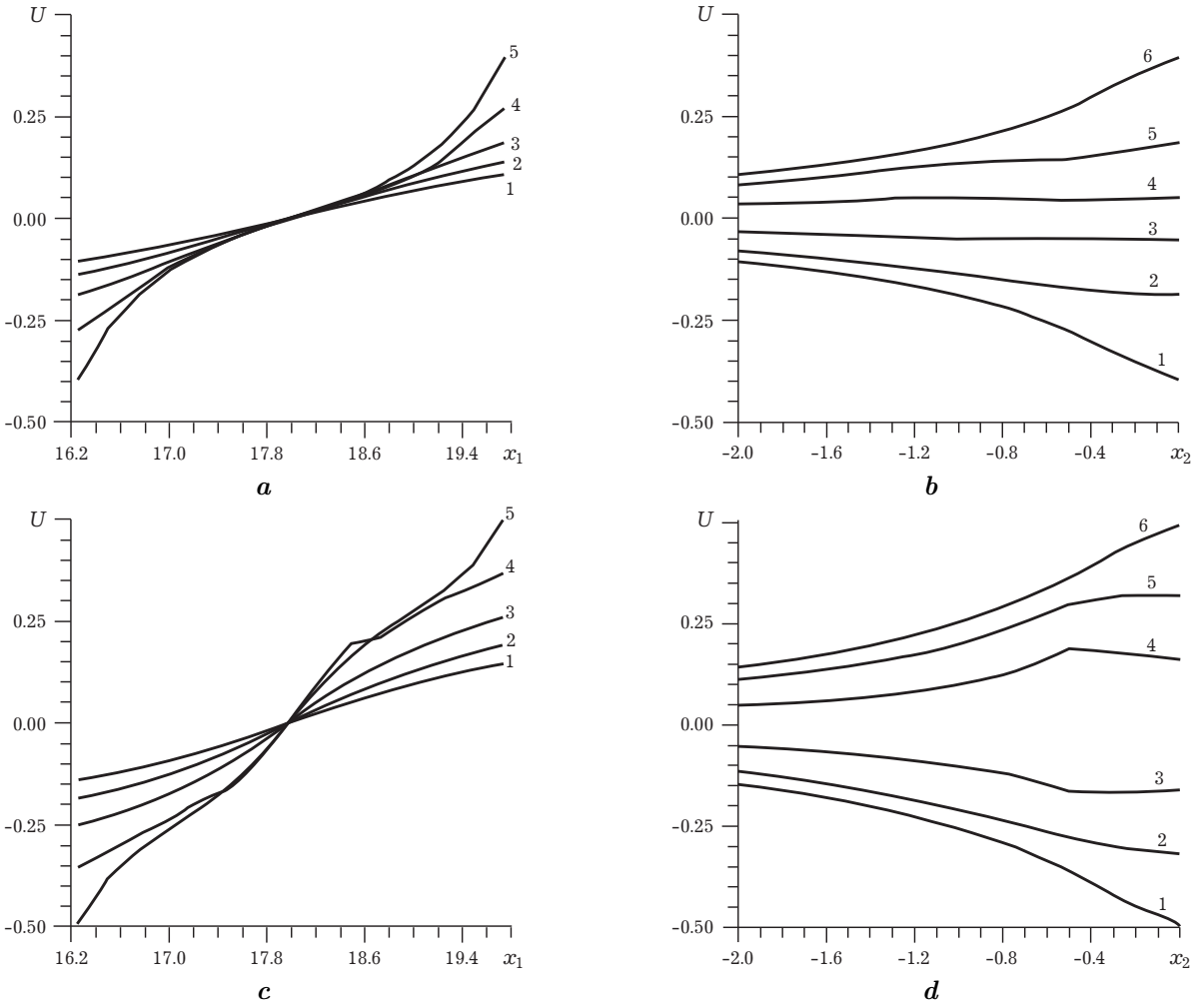

Fig. 3. Dependence of the electric potential u on the coordinate x_1 for different values x_2: 1 — -2.0, 2 — -1.5, 3 — -1.0, 4 — -0.5, 5 — 0 (***a***, ***c***) and on the coordinate x_2 for of different x_1: 1 — 16.25, 2 — 16.75, 3 — 17.5, 4 — 18.5, 5 — 19.25, 6 — 19.75 (***b***, ***d***) at $x_\sigma = 1$ (***a***, ***b***) and $k_\sigma = -0.9$ (***c***, ***d***).

7. Conclusion

An effective approach has been developed for inclusions with characteristics that are continuously dependent on the coordinates. This approach allows us to calculate the potential and its normal derivative in inhomogeneous media with curvilinear media interfaces. It is based on the combined use of the advantages of analytical and numerical methods and includes the FS (or Green function) of Laplace equations, the non-classical finite difference method only in the area of local inhomogeneity. The main ideas of such methods: splitting, near-boundary elements, contact elements and collocation.

The high accuracy of the obtained solutions within homogeneous zones is achieved by using fundamental solutions or Green functions, and at the media interfaces and in the area of local heterogeneity is ensured by numerical algorithms based on the proposed approach. The latter use the approximation of curvilinear boundaries by quadratic or cubic elements; non-uniform patterns of a finite-difference grid only in the area of inhomogeneity and interpolation of the unknown functions by high-order splines.

The effects of "compression–tension" and torsion observed as a result of the computational experiment can be used when solving inverse problems of geoelectrical prospecting to choose the correct initial approximations.

Mathematical modeling of potential fields by the developed approach is advisable and promising to use for the choice of a rational complex of electrometric observations and its successful application for the study of complex geological media, in particular, oil and gas deposits. The use of the contact

elements on the interface instead of boundary or near-boundary elements made it possible to automatically satisfy the first contact condition (potential equality) and consequently to increase the accuracy of calculations.

Numerical experiments were conducted to testify to the feasibility of the developed approach for the detection of alien inclusions in the objects using potential fields. It can be used to solve direct problems in various applied fields of mathematical physics: geophysics, materials science and defectoscopy. In particular, when it is necessary to know the distribution of temperature or electric fields in objects, when searching for minerals or to ensure the reliable operation of structures, made from materials with different characteristics. The proposed approach can be the basis for solving inverse problems of geophysics and technical diagnostics, that is, to create methods for recognizing alien inclusions, to determine their thermal or electrical conductivity, and magnetic permeability, size and location.

[1] Dmitriev V. I., Nesmeyanova N. I. Integral equation method in three-dimensional problems of low-frequency electrodynamics. Computational Mathematics and Modeling. **3**, 313–317 (1992).

[2] Zhdanov M. S., Dmitriev V. I., Gribenko A. V. Integral electric current method in 3-D electromagnetic modeling for large conductivity contrast. IEEE Transactions on Geoscience and Remote Sensing. **45** (5), 1282–1290 (2007).

[3] Banerjee P. K., Butterfield R. Boundary Element Methods in Engineering Science. London, McGraw-Hill (1981).

[4] Brebbia C. A., Telles J. C. F., Wrobel L. C. Boundary Element Techniques. Theory and Applications in Engineering. Springer-Verlag, Berlin – Heidelberg – New York – Tokyo (1984).

[5] Mukanova B., Modin I. The Boundary Element Method in Geophysical Survey. Springer, Cham (2018).

[6] Najarzadeh L., Movahedian B., Azhari M. Numerical solution of scalar wave equation by the modified radial integration boundary element method. Engineering Analysis with Boundary Elements. **105**, 267–278 (2019).

[7] Zhang Y., Qu W., Chen J. A new regularized BEM for 3D potential problems. SCIENTIA SINICA Physica, Mechanica & Astronomica. **43** (3), 297–308 (2013).

[8] Zhang J., Weicheng L., Yunqiao D., Chuanming J. A double-layer interpolation method for implementation of BEM analysis of problems in potential theory. Applied Mathematical Modelling. **51**, 250–269 (2017).

[9] Zhuravchak L. Computation of pressure change in piecewise-homogeneous reservoir for elastic regime by indirect near-boundary element method. 2019 IEEE 14th International Conference on Computer Sciences and Information Technologies (CSIT). 141–144 (2019).

[10] Zhuravchak L. M., Zabrodska N. V. Using of partly-boundary elements as a version of the indirect near-boundary element method for potential field modeling. Mathematical Modeling and Computing. **8** (1), 1–10 (2021).

[11] Zhuravchak L. Combination of near-boundary and contact elements in modeling stationary processes in piecewise-homogeneous objects. 2020 IEEE 15th International Conference on Computer Sciences and Information Technologies (CSIT). 411–414 (2020).

[12] Zhuravchak L. M., Zabrodska N. V. Nonstationary thermal fields in inhomogeneous materials with nonlinear behavior of the components. Materials Science. **46** (1), 36–46 (2010).

[13] Zhuravchak L. M., Kruk O. S. Consideration of the nonlinear behavior of environmental material and a three-dimensional internal heat sources in mathematical modeling of heat conduction. Mathematical Modeling and Computing. **2** (1), 107–113 (2015).

[14] Anshuman A., Eldho T. I. Coupled flow and transport simulation involving rate-limited adsorption in highly heterogeneous unconfined aquifers using a local strong form meshless method. Engineering Analysis with Boundary Elements. **145**, 1–12 (2022).

[15] Habibirad A., Hesameddini E., Shekari Y. A suitable hybrid meshless method for the numerical solution of time-fractional fourth-order reaction–diffusion model in the multi-dimensional case. Engineering Analysis with Boundary Elements. **145**, 149–160 (2022).

[16] Qu W., Chen W., Fu Z. Solutions of 2D and 3D non-homogeneous potential problems by using a boundary element-collocation method. Engineering Analysis with Boundary Elements. **60**, 2–9 (2015).

Моделювання потенціального поля поєднанням приграничних та контактних елементів з некласичними скінченними різницями в неоднорідному середовищі

Журавчак Л. М.

Національний університет "Львівська політехніка",
вул. С. Бандери, 12, 79013, Львів, Україна

У статті наведено узагальнену схему для знаходження розв'язків задач теорії потенціалу в двовимірних кусково-однорідних середовищах, які містять локальні області з залежними від координат фізичними характеристиками. Для опису додаткового впливу цих локальних областей, поряд з непрямими методами приграничних і контактних елементів, використано некласичний метод скінченних різниць, який базується на асиметричних скінченно-різницевих співвідношеннях. Проведено програмну реалізацію розробленого підходу для знаходження потенціалу електричного поля постійного струму в гірському неоднорідному хребті.

Ключові слова: *непрямий метод приграничних елементів; непрямий метод контактних елементів; кусково-однорідний об'єкт; локальна область неоднорідності матеріалу; некласичні скінченні різниці; електричне профілювання; двовимірна задача теорії потенціалу.*